

Nuclear cluster structure effect on elliptic and triangular flows in heavy-ion collisions

S. Zhang,¹ Y. G. Ma,^{1,2,3,*} J. H. Chen,¹ W. B. He,⁴ and C. Zhong¹

¹Shanghai Institute of Applied Physics, Chinese Academy of Sciences, Shanghai 201800, China

²University of Chinese Academy of Sciences, Beijing 100049, China

³ShanghaiTech University, Shanghai 200031, China

⁴Institute of Modern Physics, Fudan University, Shanghai 200433, China

(Received 30 January 2017; revised manuscript received 30 April 2017; published 14 June 2017)

The initial geometry effect on collective flows, which are inherited from initial projectile structure, is studied in relativistic heavy-ion collisions of $^{12}\text{C} + ^{197}\text{Au}$ by using a multiphase transport model (AMPT). Elliptic flow (v_2) and triangular flow (v_3) which are significantly resulted from the chain and triangle structure of ^{12}C with three- α clusters, respectively, in central $^{12}\text{C} + ^{197}\text{Au}$ collisions are compared with the flow from the Woods-Saxon distribution of nucleons in ^{12}C . v_3/v_2 is proposed as a probe to distinguish the pattern of α -clustered ^{12}C . This study demonstrates that the initial geometry of the collision zone inherited from nuclear structure can be explored by collective flow at the final stage in heavy-ion collisions.

DOI: [10.1103/PhysRevC.95.064904](https://doi.org/10.1103/PhysRevC.95.064904)

I. INTRODUCTION

Heavy-ion collision at relativistic energy provides abundant information about nuclear or partonic matter by the final state products [1–5]. The observables, such as collective flow [6–10], Hanbury Brown–Twiss (HBT) correlation [11–14], chiral electric-magnetic effects [15–18], and fluctuation [19–21], are sensitive to not only properties of the hot-dense matter but also the initial state of a pre-collision system. The initial geometrical fluctuation can significantly contribute on collective flow, which attracts some theoretical attentions. The hydrodynamical model [10,22–26] can describe the initial state fluctuation event by event and address its effect on collective flow and viscosity. A multiphase transport (AMPT) model [27–29] can present initial geometry fluctuations of partons created in Au+Au collisions and give the quantitative description of the elliptic and triangular flows. And other works [30–32] contribute a lot to the flow/eccentricity analysis method related to initial geometry fluctuations.

It was proposed that the intrinsic geometry of light nuclei can be studied in heavy-ion collisions by exploring elliptic and triangular flow formed in the collisions [33,34]. In these works the carbon is considered with 3- α and collides against a heavy nucleus at very high energies. Their calculation showed significant quantitative and qualitative differences between the α -clustered and uniform ^{12}C nucleus occurring in some quantities such as the triangular flow and its event-by-event fluctuations, or the correlations of the elliptic and triangular flows. Since the α cluster model was proposed by Gamow [35], α -clustering light nuclei have been studied for more than four decades [36–38] and experimental evidences for clustering from fragmentation can be found in Ref. [39]. Light $4N$ nuclei from ^{12}C to ^{28}Si were investigated in the α -clustering model of Margenau, Bloch, and Brink [40]. Recently it was proposed that the giant dipole resonance [41,42] and photonuclear reaction [43,44] can be taken as useful probes of α -clustering

configurations in ^{12}C and ^{16}O by some of the authors. Many theoretical studies suggest that ^{12}C could exhibit triangular or chain distribution of three α clusters and ^{16}O can emerge as kite, chain, square, or tetrahedron arrangements of four α clusters.

In this work, elliptic and triangular flow are studied in $^{12}\text{C} + ^{197}\text{Au}$ collisions at $\sqrt{s_{NN}} = 10$ and 200 GeV by using the AMPT model [45]. The initial nucleon distributions in ^{12}C and ^{197}Au are initialized by Woods-Saxon shapes from the HIJING model [46,47] in an original version of AMPT. And ^{12}C is configured with three- α clusters arranged in chain or triangle structure by using the results from an extended quantum molecular dynamics model (EQMD) [41–43] for investigating the effect on collective flow from initial geometrical distribution of nucleons, i.e., probing the effects of α clusters.

The paper is organized in following. Section II gives the model and methodology for briefly introducing the AMPT and EQMD models as well as the flow calculation methods. Results and discussion are given in Sec. III where the elliptic (v_2) and triangular (v_3) flows are discussed in different collision stages, and the coordinate eccentricities (ϵ_n) are demonstrated. Furthermore, the transformation coefficient from the coordinate anisotropy to momentum anisotropy is presented, and the ratio of v_3/v_2 is proposed as a probe for the clustering structure. Finally, the conclusion is drawn in Sec. IV.

II. MODEL AND METHODOLOGY

A multiphase transport model (AMPT) [45] is employed to study the effect on collective flow from the initial geometry distribution of nucleons. AMPT has been extensively applied to simulate heavy-ion collisions in a wide colliding energy range from the CERN Super Proton Synchrotron (SPS) to the CERN Large Hadron Collider (LHC), which contains the initial conditions from the HIJING model [46,47], partonic interactions modelled by a parton cascade model (ZPC) [48], hadronization in a simple quark coalescence model, and hadronic rescattering simulated by a relativistic transport

*Corresponding author: ygma@sinap.ac.cn

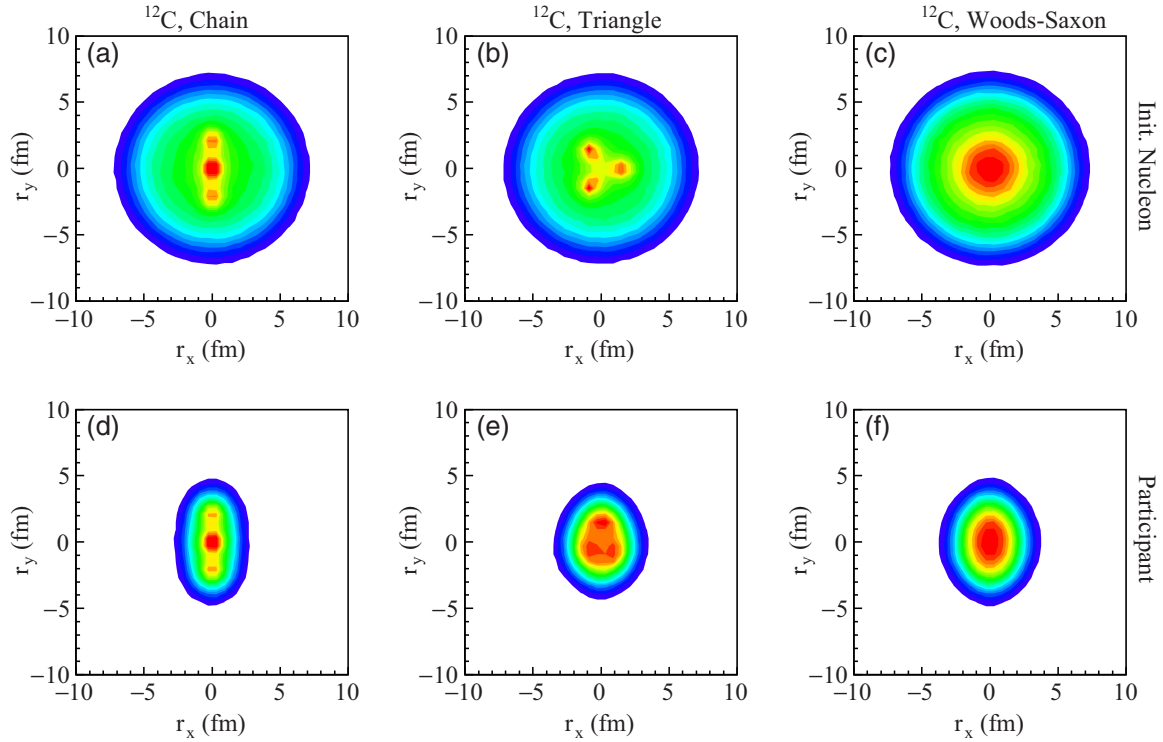


FIG. 1. In the most central collisions, initial intrinsic nucleon distribution of the $^{12}\text{C} + ^{197}\text{Au}$ system (upper panels), and the participant distributions (lower panels): (a) and (d) for the ^{12}C with the chain α -clustering structure, (b) and (e) for the triangle α -clustering structure, (c) and (f) for the Woods-Saxon nucleon distribution. The nucleon distribution in ^{197}Au always take the Woods-Saxon form.

(ART) model [49]. AMPT is successful to describe physics in relativistic heavy-ion collision for the BNL Relativistic Heavy Ion Collider (RHIC) [45] and the LHC energies [50], including pion-pair correlations [51], dihadron azimuthal correlations [52] as well as collective flow, etc. [53,54].

On the other hand, the EQMD model [55,56] was extended from the quantum molecular dynamics (QMD) [57] type models, which have successfully described physics in low energy heavy-ion reaction, e.g., collective flows, multifragmentation, HBT correlation, nuclear stopping, shear viscosity, giant resonances, and pion azimuthal asymmetry [58–66]. Due to an effective Pauli potential employed, the EQMD model can give reasonable α -cluster configurations for $4N$ nuclei. All the α -cluster configurations are different by their local minima states, with low excited energy. The parameters for configuring the α -clustered ^{12}C are inherited from the EQMD calculation [41–43]. The initial nucleon distribution in ^{12}C is configured for three cases, as shown in Fig. 1: (a) three α clusters in chain structure, (b) three α clusters in triangle structure, and (c) nucleons in Woods-Saxon distribution from HIJING model [46,47] (Woods-Saxon). The distribution of the radial center of the α clusters in ^{12}C is assumed to be a Gaussian function, $e^{-0.5(\frac{r-r_c}{\sigma_{r_c}})^2}$, here r_c is the average radial center of an α cluster and σ_{r_c} is the width of the distribution. And the nucleon inside each α cluster will be given by Woods-Saxon distribution. The parameters of r_c and σ_{r_c} can be obtained from the EQMD calculation [41–43]. For the triangle structure, $r_c = 1.8$ fm and $\sigma_{r_c} = 0.1$ fm. For the chain structure, $r_c = 2.5$ fm, $\sigma_{r_c} = 0.1$ fm for two α clusters, and the other one will be at the center in ^{12}C .

Once the radial center of the α cluster is determined, the centers of the three clusters will be placed in an equilateral triangle for the triangle structure or in a line for the chain structure. For the nucleons in ^{197}Au , we just take the Woods-Saxon distribution from the HIJING model [46,47] (Woods-Saxon). Figure 1(a), 1(b), and 1(c) shows the three cases of intrinsic initial nucleon distribution of the $^{12}\text{C} + ^{197}\text{Au}$ system in the most central collisions. And the intrinsic participant distributions are shown in Fig. 1(d), 1(e), and 1(f), respectively, for the chain, triangle, and Woods-Saxon distribution initialized ^{12}C in $^{12}\text{C} + ^{197}\text{Au}$ collisions in the AMPT model. From Fig. 1(d), 1(e), and 1(f), we can see that the participant distribution inherits the geometrical shape of the initialized ^{12}C . The coordinate asymmetry will be transferred to momentum space asymmetry in the evolution of the fireball created in the collisions from hydrodynamical theory [67,68].

With these intrinsic nucleon distributions of each configuration, the orientation of all nucleons is rotated randomly for each event in heavy ion collisions. After accumulating enough events for statistics, the observables are obtained. Figure 2(a) and 2(b) presents the distribution of the number of tracks (particles) (N_{track}) in collisions for the three ^{12}C configuration cases, namely the Woods-Saxon, triangle, and chain structures. Noting that the N_{track} is calculated in the rapidity window ($-2 < y < 2$) and transverse momentum window ($0.2 < p_T < 6$) GeV/c for the charged pions (π^\pm), kaons (K^\pm), and protons (p and \bar{p}). Figure 2(c) and 2(d) shows average N_{track} ($\langle N_{\text{track}} \rangle$) as a function of impact parameter b of ^{12}C and ^{197}Au . From Fig. 2(a) and 2(c),

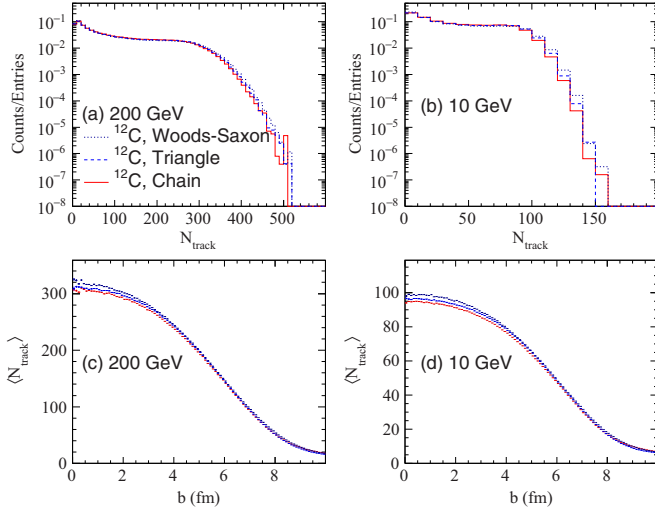


FIG. 2. The N_{track} distribution in $^{12}\text{C} + ^{197}\text{Au}$ collisions at $\sqrt{s_{NN}} = 200$ GeV (a) and 10 GeV (b), respectively; Average N_{track} ($\langle N_{\text{track}} \rangle$) as a function of impact parameter b at (c) 200 GeV and (d) 10 GeV, respectively.

and 2(b) and 2(d), the most central collisions can be estimated in impact parameter $b < 2$ fm with $N_{\text{track}} > 280$ at $\sqrt{s_{NN}} = 200$ GeV and $N_{\text{track}} > 90$ at $\sqrt{s_{NN}} = 10$ GeV. From the figure, it can be seen that there is no significant difference for total track numbers among three cases for ^{12}C initialization.

The collective properties in heavy-ion collisions can be investigated by the azimuthal anisotropy of detected particles [69]. The final-state particle azimuthal distribution can be expanded as [70]

$$E \frac{d^3 N}{d^3 p} = \frac{1}{2\pi} \frac{d^2 N}{p_T dp_T dy} \left(1 + \sum_{i=1}^N 2v_n \cos[n(\phi - \Psi_{RP})] \right), \quad (1)$$

where E is the energy, p_T is transverse momentum, y is rapidity, and ϕ is azimuthal angle of the particle. Ψ_{RP} is the reaction plane angle. The Fourier coefficients v_n ($n = 1, 2, 3, \dots$) represent the collective flow of different orders in azimuthal anisotropies with the form

$$v_n = \langle \cos(n[\phi - \Psi_{RP}]) \rangle, \quad (2)$$

where the bracket $\langle \rangle$ denotes statistical averaging over particles and events. Harmonic flow v_n can also be calculated through participant plane angle $\Psi_n\{PP\}$ instead of reaction plane Ψ_{RP} . In the participant coordinate system, the participant plane angle $\Psi_n\{PP\}$ can be obtained event by event using the following equation [27,30–32,71]:

$$\Psi_n\{PP\} = \frac{\text{atan2}(\langle r^2 \sin(n\phi_P) \rangle, \langle r^2 \cos(n\phi_P) \rangle) + \pi}{n}, \quad (3)$$

where $\Psi_n\{PP\}$ is the n th-order participant plane angle, r and ϕ_P are coordinate position and azimuthal angle of participants in the collision zone at initial state, and the average $\langle \dots \rangle$ denotes density weighting. Then the harmonic flow coefficients with respect to participant plane can be

defined as

$$v_n \equiv \langle \cos(n[\phi - \Psi_n\{PP\}]) \rangle. \quad (4)$$

Also, the initial coordinate anisotropies can be quantified as participant eccentricity coefficients [27,30–32]

$$\epsilon_n\{PP\} \equiv \frac{\sqrt{\langle r^2 \cos(n\phi_P) \rangle^2 + \langle r^2 \sin(n\phi_P) \rangle^2}}{\langle r^2 \rangle}. \quad (5)$$

The collisions are initialized by the HIJING model [46,47] in AMPT model. Since the initial fluctuation should be taken into account, the initial coordinates to calculate Eq. (4) and (5) will be provided by the HIJING process in this work.

This method (participant plane method) has been used to calculate collective flow in different models [22–25,27–32]. And it was always applied to discuss the initial geometric fluctuation effect on collective flow because the participant plane angle $\Psi_n\{PP\}$ is constructed by initial energy distribution in coordinate space with the event-by-event fluctuation effects. In this work, the event-by-event participant plane method for flow calculation is employed to calculate elliptic flow v_2 and triangular flow v_3 in $^{12}\text{C} + ^{197}\text{Au}$ collisions at $\sqrt{s_{NN}} = 10$ GeV and 200 GeV in the AMPT model. And a probe to distinguish different α -clustering structures of ^{12}C will be proposed from the results of elliptic flow v_2 and triangular flow v_3 .

III. RESULTS AND DISCUSSION

Figures 3 and 4 present elliptic flow (v_2) and triangular flow (v_3) as a function of N_{track} in $^{12}\text{C} + ^{197}\text{Au}$ collisions at $\sqrt{s_{NN}} = 200$ GeV and 10 GeV in the AMPT model with different configured pattern of ^{12}C . The initial partons inherited from the HIJING [46,47] model are considered as the initial stage of the collisions. From Figs. 3(a), 3(e) and 4(a), 4(e), there is no elliptic flow v_2 and triangular flow v_3 in the initial stage of the collision system at both $\sqrt{s_{NN}} = 200$ GeV and 10 GeV. The initial partons will interact with each other and then reach freeze-out status, which is simulated by the ZPC model [48]. After the parton interaction simulation in the ZPC model, v_2 and v_3 are formed as shown in Figs. 3(b), 3(f) and 4(b), 4(f). It is obvious that the developed elliptic flow is larger for the chain structure than for other patterns of ^{12}C and the developed triangular flow is more significant for the triangle structure than for other patterns of ^{12}C at both $\sqrt{s_{NN}} = 200$ GeV and 10 GeV. This is consistent with the view from hydrodynamical theory [10,67,68] that collective flow results from the initial coordinate asymmetry. The freeze-out partons are converted to hadrons through a naive coalescence model [45] and here these hadrons do not yet participate in hadronic rescattering. Figures 3(c), 3(g) and 4(c), 4(g) show elliptic flow and triangular flow of hadrons without hadronic rescattering. The formed hadrons will experience hadronic interaction simulated by the ART [49] model. The elliptic flow and triangular flow of hadrons with hadronic rescattering are shown in panels (d) and (h) in Figs. 3 and 4, respectively. It is seen that there is no significant contribution on collective flow from hadronic rescattering by comparing the flows of hadrons with and without hadronic rescattering. The collective flow of hadrons with/without

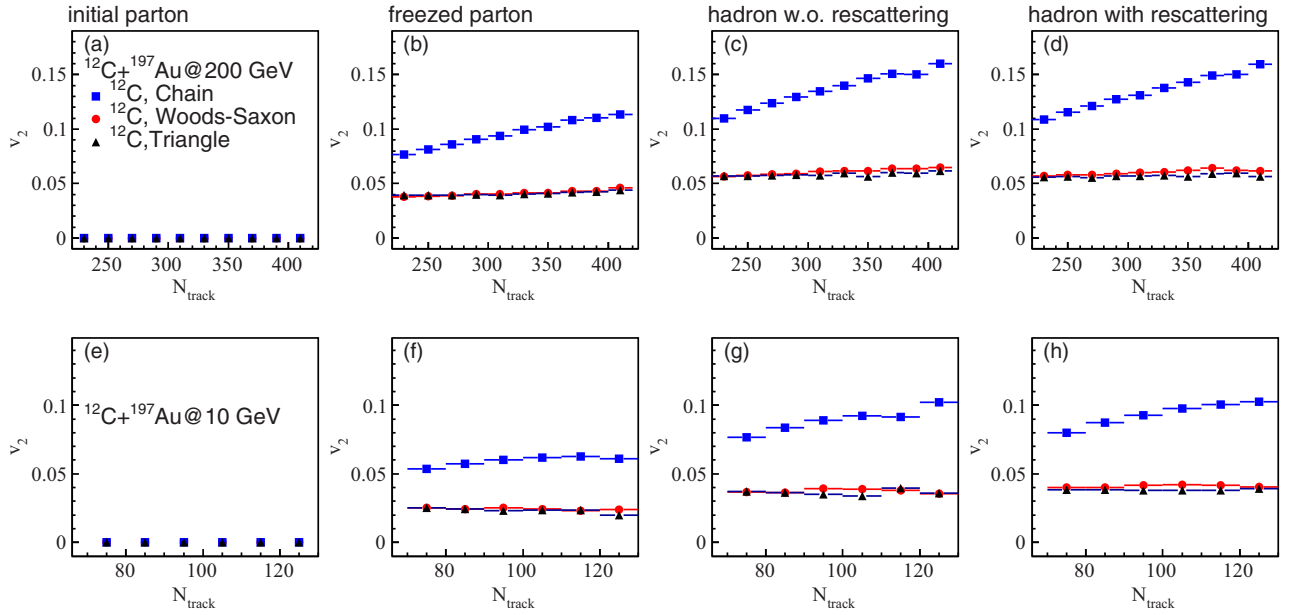


FIG. 3. In $^{12}\text{C} + ^{197}\text{Au}$ collisions at $\sqrt{s_{NN}} = 200$ GeV (upper panels) and 10 GeV (lower panels), v_2 as function of N_{track} : (a) and (e) for initial partons, (b) and (f) for the freeze-out partons, (c) and (g) for the hadrons without hadronic rescattering, and (d) and (h) for the final-state hadrons.

hadronic rescattering is larger than that of the freeze-out parton because of the coalescence mechanism, which brings out the number of constituent quark (NCQ) scaling of collective flow [29,72] and also NCQ scaling of nuclear modification factor R_{cp} of the hadron [73]. Here, the calculations are performed in a transverse momentum window of $0 < p_T < 1.5\text{GeV}/c$ for partons and $0 < p_T < 3\text{GeV}/c$ for hadrons, with a midrapidity window $-1 < y < 1$. Since we mainly discuss the relationship between initial geometry distribution and final momentum distribution, eccentricity coefficients are calculated by using initial partons inherited from the HIJING

[46,47] and collective flow from hadrons with hadronic rescattering.

Now we move to discuss the initial geometry effect on collective flows. From the above discussion, we can only conclude that the chain structure of α clusters mainly contributes to elliptic flow v_2 while the triangle structure significantly contributes to triangular flow v_3 . It will be useful for experimental analysis if there is a probe to distinguish the geometry pattern of ^{12}C through collective flow measurement. In Refs. [33,34], the collective flow ratio between the flow from four-particle cumulant and the flow from two-particle

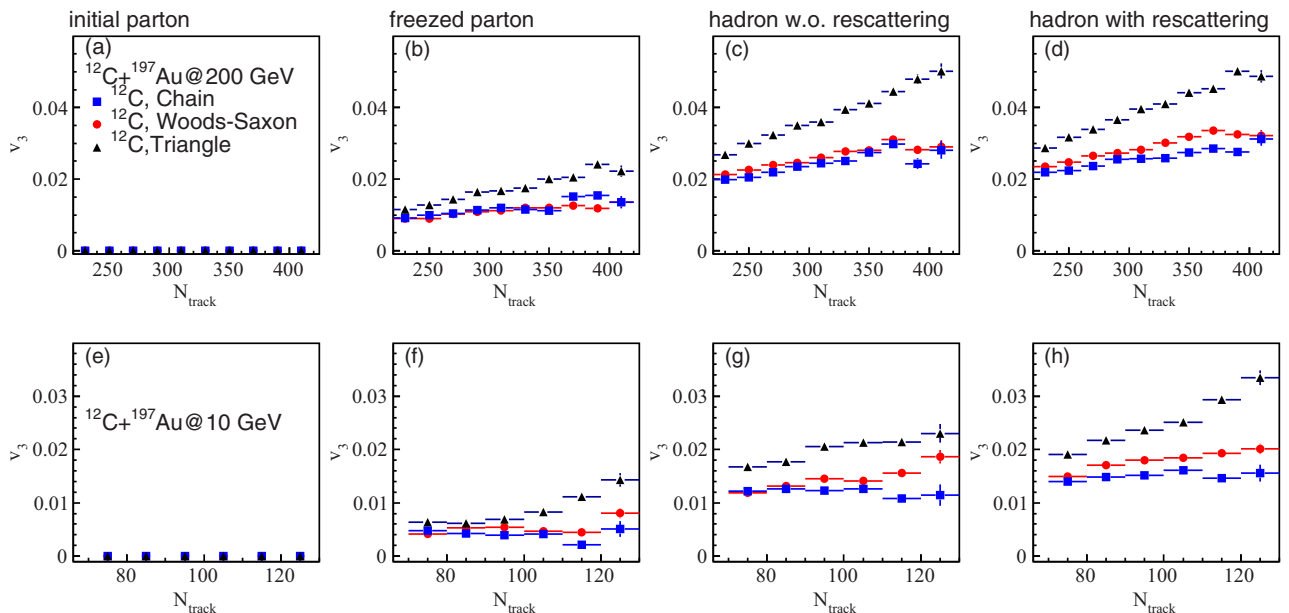


FIG. 4. Same as Fig. 3 but for v_3 .

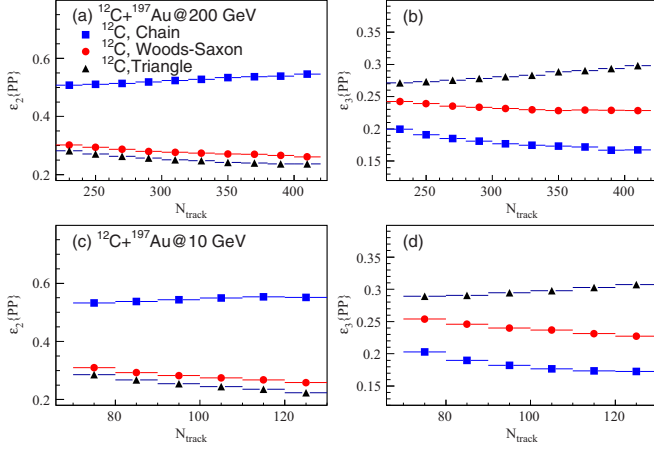


FIG. 5. In $^{12}\text{C} + ^{197}\text{Au}$ collisions at $\sqrt{s_{NN}} = 200$ GeV (upper panels) and 10 GeV (lower panels), second- and third-order participant eccentricity coefficients, (a) and (c) for $\epsilon_2\{PP\}$, (b) and (d) for $\epsilon_3\{PP\}$, as function of N_{track} .

cumulant is proposed as a signature of α -clustered ^{12}C . In this work another observable will be presented to distinguish the geometry pattern of ^{12}C .

Figure 5 presents the second- and third-order participant eccentricity coefficients, namely $\epsilon_2\{PP\}$ and $\epsilon_3\{PP\}$, as a function of N_{track} in $^{12}\text{C} + ^{197}\text{Au}$ collisions at $\sqrt{s_{NN}} = 200$ GeV and 10 GeV in the AMPT model with a different configuration pattern of ^{12}C . $\epsilon_2\{PP\}$ slightly increases for the chain structure pattern of ^{12}C and decreases for the other patterns, with the increasing of N_{track} . So does for $\epsilon_3\{PP\}$. The N_{track} dependence of $\epsilon_2\{PP\}$ and $\epsilon_3\{PP\}$ is similar at $\sqrt{s_{NN}} = 200$ GeV as well as 10 GeV.

The hydrodynamical calculation suggested how the initial geometry distribution (fluctuation) transforms into final flow observables in a heavy-ion collision [10,74,75]. And the relationship between initial geometry eccentricity coefficients and flow coefficients are as

$$v_n = \kappa_n \epsilon_n, n = 2, 3. \quad (6)$$

The response coefficients κ_n show the efficiency of the transformation from initial geometry distribution to momentum space in collisions. As discussed in Ref. [33], κ_n depends on the details of the collision system and model, the linearity of Eq. (6) allows for model-independent studies for collective flow.

Figure 6 presents v_2/ϵ_2 and v_3/ϵ_3 in panels (a), (b) and (c), (d) at $\sqrt{s_{NN}} = 200$ and 10 GeV, respectively. The ratio of v_n/ϵ_n ($n = 2, 3$) increases with N_{track} in different p_T range and collisions energy. In the low p_T range ($0 < p_T < 1\text{GeV}/c$), v_n/ϵ_n ($n = 2, 3$) nearly keep in the same line for the triangle structure, chain structure, and Woods-Saxon distributions, and show almost independent of N_{track} . In other words, there exists the same efficiency of the transformation from initial geometry distribution to momentum space for the three different configuration structures of ^{12}C colliding against ^{197}Au in the low p_T range. In the higher p_T range ($1 < p_T < 3\text{GeV}/c$), however, there are little differences of v_n/ϵ_n ($n = 2, 3$) among different cases of configuration structures of ^{12}C , the chain

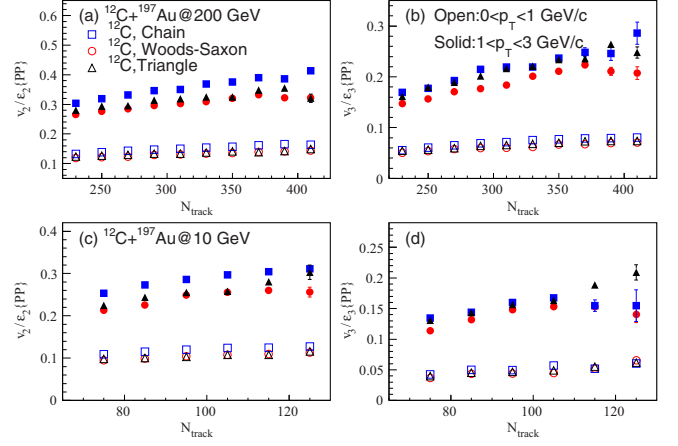


FIG. 6. In $^{12}\text{C} + ^{197}\text{Au}$ collisions at $\sqrt{s_{NN}} = 200$ GeV (upper panels) and 10 GeV (lower panels), (a) and (c) $v_2/\epsilon_2\{PP\}$, (b) and (d) $v_3/\epsilon_3\{PP\}$ of final hadrons as function of N_{track} .

structure shows a little higher value than the other cases. Also, all v_n/ϵ_n ($n = 2, 3$) display a slight increasing with the N_{track} . Therefore, for higher p_T hadrons, there are different transformation efficiencies from initial phase space to final state for the three different configurations.

From the above discussion, we know that the initial geometry asymmetry can be transported to momentum space and remains observed by elliptic and triangular flows. Figure 7(a) and 7(c) shows the ratio of $\epsilon_3\{PP\}/\epsilon_2\{PP\}$ as a function of N_{track} in $^{12}\text{C} + ^{197}\text{Au}$ collisions at $\sqrt{s_{NN}} = 200$ and 10 GeV, respectively, with a different configured pattern of ^{12}C . The values of $\epsilon_3\{PP\}/\epsilon_2\{PP\}$ show a drop according to the order of the triangle structure, Woods-Saxon, and chain structure patterns of ^{12}C . It is interesting that the ratios of v_3/v_2 of the final hadrons take the similar order as $\epsilon_3\{PP\}/\epsilon_2\{PP\}$, as shown in Fig. 7(b) and 7(d). $\epsilon_3\{PP\}/\epsilon_2\{PP\}$ and v_3/v_2 all show an increasing dependent trend with the increasing of N_{track} in the triangle structure pattern of ^{12}C and approximately keep flat in the other two patterns not only at low p_T but also in the higher p_T region.

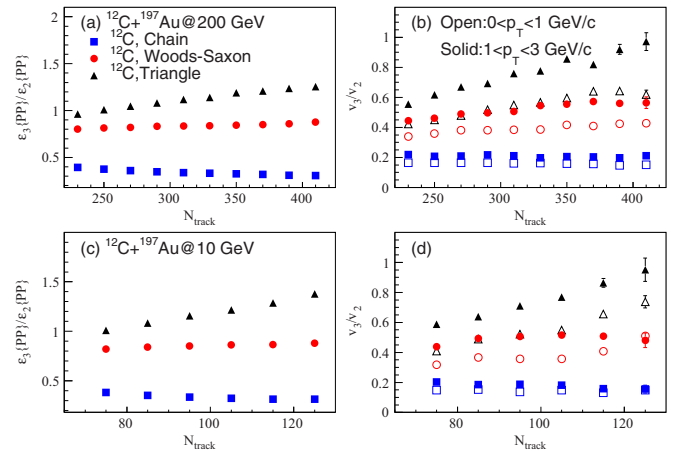


FIG. 7. In $^{12}\text{C} + ^{197}\text{Au}$ collisions at $\sqrt{s_{NN}} = 200$ GeV (upper panels) and 10 GeV (lower panels), (a) and (c) $\epsilon_3\{PP\}/\epsilon_2\{PP\}$, (b) and (d) v_3/v_2 of final hadrons as function of N_{track} .

Therefore the ratio of v_3/v_2 is proposed as a probe to distinguish the α -clustering structure pattern of ^{12}C in experiment. Especially, we can consider a nucleus without exotic structure near the ^{12}C nucleus or an isobar nucleus of ^{12}C to collide against a heavy ion as a reference system. If v_3/v_2 in $^{12}\text{C} + ^{197}\text{Au}$ collisions is obviously larger than that in the reference system, ^{12}C could be constructed by the three α -clusters triangle structures. If v_3/v_2 in the $^{12}\text{C} + ^{197}\text{Au}$ collision is significantly smaller than that in the reference system, ^{12}C can be constructed from the three α -clusters chain structure. If v_3/v_2 in the $^{12}\text{C} + ^{197}\text{Au}$ collision is comparable with that in the reference system, ^{12}C should be a nonexotic structure nucleus. And the sharp increasing trend of v_3/v_2 as a function of N_{track} can be seen as a probe to distinguish if ^{12}C is formed in triangle shape with three α s or not.

In the above results, collective flows and initial geometry coefficients at $\sqrt{s_{NN}} = 200$ GeV and 10 GeV are presented. However, we did not discuss too much the energy dependence of these results since there is no significant difference in the centrality dependence of the flows and initial geometry coefficients between $\sqrt{s_{NN}} = 200$ GeV and 10 GeV. We should note that the multiplicity is higher at $\sqrt{s_{NN}} = 200$ GeV than at $\sqrt{s_{NN}} = 10$ GeV and from this point the measurements for collective flows will be more feasible at $\sqrt{s_{NN}} = 200$ GeV from different methods such as the reaction plane method and Q -cumulant method.

IV. SUMMARY

In summary, the chain and triangle α -clustered as well as the Woods-Saxon distribution pattern of ^{12}C colliding against ^{197}Au are calculated at $\sqrt{s_{NN}} = 200$ GeV and 10 GeV in the AMPT model. The effects on collective flow from initial geometry of nucleon distribution are discussed in this work. The pattern of the chain arranged α cluster significantly contributes on elliptic flow v_2 but the triangle arranged α -cluster pattern mainly enlarges triangular flow v_3 . This is consistent with the viewpoint from hydrodynamical theory on collective flow that the initial geometry asymmetry will be transformed to momentum space at final state. And v_3/v_2 is proposed as a probe to distinguish the pattern of α -clustered ^{12}C for experimental analysis.

ACKNOWLEDGMENTS

We are grateful for discussion with Dr. Aihong Tang from BNL. This work was supported in part by the National Natural Science Foundation of China under Contracts No. 11421505, No. 11220101005, No. 11105207, No. 11275250, No. 11322547, and No. U1232206, the Major State Basic Research Development Program in China under Contract No. 2014CB845400, and the Key Research Program of Frontier Sciences of the CAS under Grant No. QYZDJ-SSW-SLH002.

-
- [1] I. Arsene *et al.* (BRAHMS Collaboration), *Nucl. Phys. A* **757**, 1 (2005).
- [2] B. B. Back *et al.* (PHOBOS Collaboration), *Nucl. Phys. A* **757**, 28 (2005).
- [3] J. Adams *et al.* (STAR Collaboration), *Nucl. Phys. A* **757**, 102 (2005).
- [4] K. Adcox *et al.* (PHENIX Collaboration), *Nucl. Phys. A* **757**, 184 (2005).
- [5] B. Müller, J. Schukraft, and B. Wyslouch, *Annu. Rev. Nucl. Part. Sci.* **62**, 361 (2012).
- [6] L. Adamczyk *et al.* (STAR Collaboration), *Phys. Rev. C* **88**, 014902 (2013).
- [7] L. Adamczyk *et al.* (STAR Collaboration), *Phys. Rev. Lett.* **112**, 162301 (2014).
- [8] L. Adamczyk *et al.* (STAR Collaboration), *Phys. Rev. C* **88**, 014904 (2013).
- [9] L. Adamczyk *et al.* (STAR Collaboration), *Phys. Rev. Lett.* **114**, 252302 (2015).
- [10] For a review, see, e.g., H. C. Song, Y. Zhou, and K. Gajdošová, *Nucl. Sci. Tech.* **28**, 99 (2017).
- [11] L. Adamczyk *et al.* (STAR Collaboration), *Phys. Rev. C* **92**, 014904 (2015).
- [12] A. Adare *et al.* (PHENIX Collaboration), [arXiv:1410.2559](https://arxiv.org/abs/1410.2559).
- [13] J. Yang and W. N. Zhang, *Nucl. Sci. Tech.* **27**, 147 (2016).
- [14] R. A. Lacey, *Phys. Rev. Lett.* **114**, 142301 (2015).
- [15] D. E. Kharzeev, L. D. McLerran, and H. J. Warringa, *Nucl. Phys. A* **803**, 227 (2008).
- [16] G. L. Ma and X. G. Huang, *Phys. Rev. C* **91**, 054901 (2015).
- [17] For a review, see, e.g., K. Hattori and X. G. Huang, *Nucl. Sci. Tech.* **28**, 26 (2017).
- [18] W.-T. Deng, X.-G. Huang, G.-L. Ma, and G. Wang, *Phys. Rev. C* **94**, 041901(R) (2016).
- [19] L. Adamczyk *et al.* (STAR Collaboration), *Phys. Rev. C* **92**, 021901(R) (2015).
- [20] C. M. Ko and F. Li, *Nucl. Sci. Tech.* **27**, 140 (2016).
- [21] For a review, see, e.g., X. F. Luo and N. Xu, [arXiv:1701.02105v1](https://arxiv.org/abs/1701.02105) [*Nucl. Sci. Tech.* **28** (2017)].
- [22] R. D. de Souza, J. Takahashi, T. Kodama, and P. Sorensen, *Phys. Rev. C* **85**, 054909 (2012).
- [23] A. K. Chaudhuri, *Phys. Lett. B* **710**, 339 (2012).
- [24] H. Song, S. A. Bass, and U. Heinz, *Phys. Rev. C* **83**, 054912 (2011).
- [25] S. Floerchinger and U. A. Wiedemann, *Phys. Lett. B* **728**, 407 (2014).
- [26] R. Peschanski and E. N. Saridakis, *Phys. Rev. C* **80**, 024907 (2009).
- [27] L. Ma, G. L. Ma, and Y. G. Ma, *Phys. Rev. C* **94**, 044915 (2016).
- [28] L. Ma, G. L. Ma, and Y. G. Ma, *Phys. Rev. C* **89**, 044907 (2014).
- [29] L. X. Han, G. L. Ma, Y. G. Ma, X. Z. Cai, J. H. Chen, S. Zhang, and C. Zhong, *Phys. Rev. C* **84**, 064907 (2011).
- [30] S. A. Voloshin, A. M. Poskanzer, A. Tang *et al.*, *Phys. Lett. B* **659**, 537 (2008).
- [31] B. Alver and G. Roland, *Phys. Rev. C* **81**, 054905 (2010).
- [32] R. A. Lacey, R. Wei, J. Jia, N. N. Ajitanand, J. M. Alexander, and A. Taranenko, *Phys. Rev. C* **83**, 044902 (2011).
- [33] P. Božek, W. Broniowski, E. R. Arriola, and M. Rybczyński, *Phys. Rev. C* **90**, 064902 (2014).
- [34] W. Broniowski and E. R. Arriola, *Phys. Rev. Lett.* **112**, 112501 (2014).
- [35] F. D. Murnaghan, *Bull. Amer. Math. Soc.* **39**, 487 (1933).

- [36] W. Greiner, J. Y. Park, and W. Scheid, *Nuclear Molecules* (World Scientific, Singapore, 1995).
- [37] W. von Oertzen, M. Freer, and Y. Kanada-Enyo, *Phys. Rep.* **432**, 43 (2006).
- [38] Y. Kanada-Enyo, M. Kimura, F. Kobayashi *et al.*, *Nucl. Sci. Tech.* **26**, S20501 (2015).
- [39] P. I. Zarubin, *Clusters in Nuclei*, Lecture Notes in Physics (Springer, New York, 2014).
- [40] D. M. Brink, H. Friedrich, A. Weiguny, and C. W. Wong, *Phys. Lett. B* **33**, 143 (1970).
- [41] W. B. He, Y. G. Ma, X. G. Cao, X. Z. Cai, and G. Q. Zhang, *Phys. Rev. Lett.* **113**, 032506 (2014).
- [42] W. B. He, Y. G. Ma, X. G. Cao, X. Z. Cai, and G. Q. Zhang, *Phys. Rev. C* **94**, 014301 (2016).
- [43] B. S. Huang, Y. G. Ma, and W. B. He, *Phys. Rev. C* **95**, 034606 (2017); *Eur. Phys. J. A* **53**, 119 (2017).
- [44] B. S. Huang and Y. G. Ma, *Chin. Phys. Lett.* **34**, 072401 (2017).
- [45] Z.-W. Lin, C. M. Ko, B.-A. Li, B. Zhang, and S. Pal, *Phys. Rev. C* **72**, 064901 (2005).
- [46] X.-N. Wang and M. Gyulassy, *Phys. Rev. D* **44**, 3501 (1991).
- [47] M. Gyulassy and X. N. Wang, *Comput. Phys. Commun.* **83**, 307 (1994).
- [48] B. Zhang, *Comput. Phys. Commun.* **109**, 193 (1998).
- [49] B. A. Li and C. M. Ko, *Phys. Rev. C* **52**, 2037 (1995).
- [50] G. L. Ma and Z. W. Lin, *Phys. Rev. C* **93**, 054911 (2016).
- [51] Z.-W. Lin, C. M. Ko, and S. Pal, *Phys. Rev. Lett.* **89**, 152301 (2002).
- [52] G. L. Ma, G. S. Zhang, Y. G. Ma *et al.*, *Phys. Lett. B* **641**, 362 (2006).
- [53] B. I. Abelev *et al.* (STAR Collaboration), *Phys. Rev. Lett.* **101**, 252301 (2008).
- [54] A. Bzdak and G. L. Ma, *Phys. Rev. Lett.* **113**, 252301 (2014).
- [55] T. Maruyama, K. Niita, and A. Iwamoto, *Phys. Rev. C* **53**, 297 (1996).
- [56] R. Wada, K. Hagel, J. Cibor *et al.*, *Phys. Lett. B* **422**, 6 (1998).
- [57] J. Aichelin, *Phys. Rep.* **202**, 233 (1991).
- [58] T. Z. Yan *et al.*, *Phys. Lett. B* **638**, 50 (2006).
- [59] Y. G. Ma and W. Q. Shen, *Phys. Rev. C* **51**, 710 (1995).
- [60] Y. G. Ma, Y. B. Wei, W. Q. Shen, X. Z. Cai, J. G. Chen, J. H. Chen, D. Q. Fang, W. Guo, C. W. Ma, G. L. Ma, Q. M. Su, W. D. Tian, K. Wang, T. Z. Yan, C. Zhong, and J. X. Zuo, *Phys. Rev. C* **73**, 014604 (2006).
- [61] G. Q. Zhang, Y. G. Ma, X. G. Cao, C. L. Zhou, X. Z. Cai, D. Q. Fang, W. D. Tian, and H. W. Wang, *Phys. Rev. C* **84**, 034612 (2011); Y. Z. Xing *et al.*, *Chin. Phys. Lett.* **33**, 122501 (2016).
- [62] Z. Q. Feng, *Nucl. Sci. Tech.* **26**, S20512 (2015).
- [63] C. L. Zhou, Y. G. Ma, D. Q. Fang, G. Q. Zhang, J. Xu, X. G. Cao, and W. Q. Shen, *Phys. Rev. C* **90**, 057601 (2014).
- [64] C. Tao, Y. G. Ma, G. Q. Zhang *et al.*, *Nucl. Sci. Tech.* **24**, 030502 (2013); *Phys. Rev. C* **87**, 014621 (2013).
- [65] J. Chen, Z. Q. Feng, and J. S. Wang, *Nucl. Sci. Tech.* **27**, 73 (2016).
- [66] T. T. Wang *et al.*, *Chin. Phys. Lett.* **32**, 062501 (2015).
- [67] J. P. Blaizot and J. Y. Ollitrault, *Nucl. Phys. A* **458**, 745 (1986).
- [68] D. Teaney and E. V. Shuryak, *Phys. Rev. Lett.* **83**, 4951 (1999).
- [69] J. Y. Ollitrault, *Phys. Rev. D* **46**, 229 (1992).
- [70] A. M. Poskanzer and S. A. Voloshin, *Phys. Rev. C* **58**, 1671 (1998).
- [71] J. Wang, Y. G. Ma, G. Q. Zhang, and W. Q. Shen, *Phys. Rev. C* **90**, 054601 (2014).
- [72] J. Tian, J. H. Chen, Y. G. Ma, X. Z. Cai, F. Jin, G. L. Ma, S. Zhang, and C. Zhong, *Phys. Rev. C* **79**, 067901 (2009).
- [73] C. S. Zhou, Y. G. Ma, and S. Zhang, *Eur. Phys. J. A* **52**, 354 (2016).
- [74] F. G. Gardim, F. Grassi, M. Luzum, and J.-Y. Ollitrault, *Phys. Rev. C* **85**, 024908 (2012).
- [75] H. Niemi, G. S. Denicol, H. Holopainen, and P. Huovinen, *Phys. Rev. C* **87**, 054901 (2013).